Journal of the Technical University of Gabrovo

https://mc04.manuscriptcentral.com/jtug

FINITE ELEMENT SIMULATIONS OF STATIC MECHANICAL SURFACE TREATMENT PROCESSES – A REVIEW AND PROSPECTS

Vladimir Dunchev*, Mariana Ichkova
Technical University of Gabrovo, 5300 Gabrovo, Bulgaria

ARTICLE INFO

Article history:
Received 14 January 2020
Accepted 29 January 2020

Keywords:
Mechanical surface treatment,
Burnishing, FE simulation

ABSTRACT

This article reviews finite element (FE) simulations of static mechanical surface treatment (MST) processes for metal components. These static burnishing methods, based on severe plastic deformations of the surface and subsurface layers, improve the surface integrity (SI) of the respective components dramatically and thus their operational properties. The finite element method (FEM) is a basic method used for numerical investigations of MST processes. Although FEM always requires experimental verification and an experiment to establish an adequate material constitutive model, this method saves the researcher significant time and resources. In this article, a comprehensive analysis of the published studies devoted to FE simulations of static MST processes has been conducted. Based on the analysis, five basic conditions have being established in order to build an adequate FE model of the static burnishing process.

1. INTRODUCTION

To improve the fatigue and tribological behavior as well as the corrosion resistance of structural components, it is necessary to modify the set of topographic, mechanical, chemical and metallurgical properties comprising the surface integrity (SI) of their surface layers. During the preparation of work-pieces, improvements in SI are practically impossible. On the other hand, real work-pieces contain many defects that cannot be ignored. Therefore, SI depends on technological process used in the production of metal structural and machine components and, to a large extent, the type of finishing treatment. Hence, mechanical surface treatment (MST) methods are particularly promising since they provide a lower cost/quality ratio. The essence of MST is the plastic deformation of the surface peaks created by the sliding friction or rolling contact between a deforming element and the surface being treated. The peaks of the relief are plastically deformed as the metal flows to the free valleys. MST methods can be either dynamic or static. The plastic deformation in the dynamic methods (shot peening, percussive burnishing and so forth) is produced by a short-term impact on the surface layers. The static methods, which are the subject of this article, find greater application in practice. In the static methods, a rotational deforming element is statically pressed against the surface to be treated as the deformation process is carried out continuously in time. The static MST methods that are most widely applied in practice are [1]:

- basic – 1) ball burnishing (BB); 2) roller burnishing (RB); and 3) slide burnishing (SB) (Fig. 1);
- hybrid – 1) RB that achieves rolling and sliding effects simultaneously; 2) BB with undefined ball motion (Fig. 2);

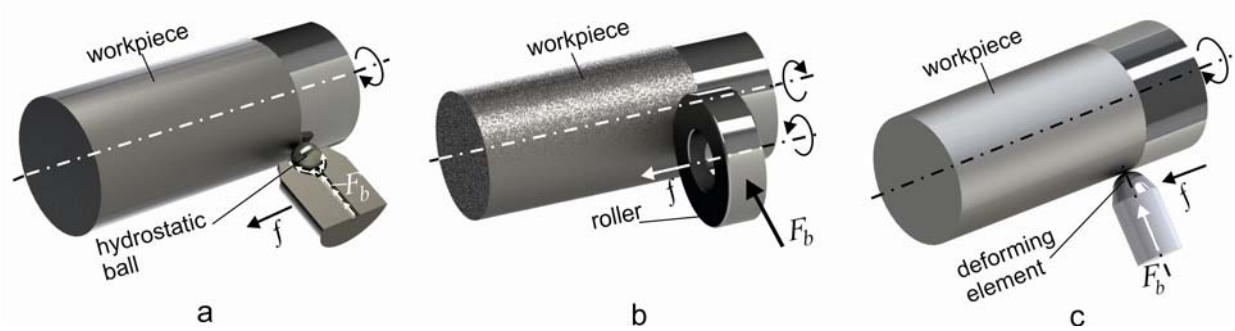

Fig. 1. Basic burnishing methods: a. ball burnishing; b. roller burnishing; c. slide burnishing

* Corresponding author. E-mail: v.dunchev@tugab.bg

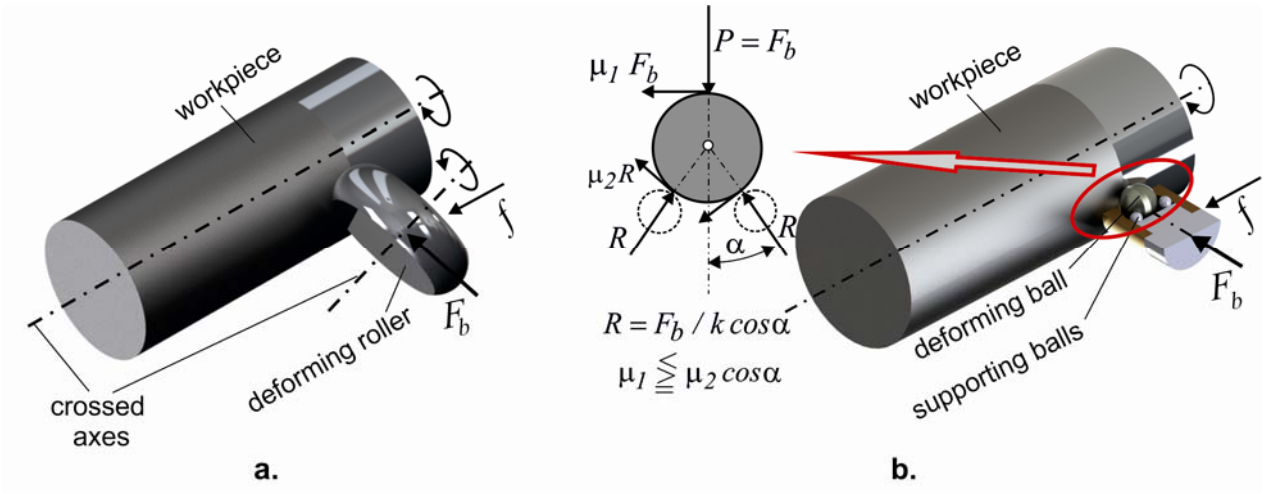

Fig. 2. Hybrid burnishing methods: a. roller burnishing that achieves simultaneously rolling and sliding effects; b. ball burnishing with undefined ball motion

● combined – 1) laser-assisted burnishing; 2) ultrasonic burnishing; 3) cryogenic burnishing.

The quantitative characteristics of the parameters of the static MST methods define the corresponding burnishing processes. The latter may be classified according to the required operational properties of the treated surfaces, as follows:

1) Smoothing burnishing, which, depending on the type of tangential contact, may consist of roller or diamond burnishing. is one of the main processes According to the multinational company Ecoroll [2], RB, which usually involves tools containing multiple rollers, is one of the main processes for the practical realization of smoothing.

2) Deep burnishing, which depending on the type of contact may consist of deep rolling (DR) (name adopted by Ecoroll) or deep SB. The DR process is carried out by a deforming sphere subjected to hydrostatic pressure or by a cylindrical or profile roller (usually with a toroidal working surface). The low plasticity burnishing (LPB) process [3, 4] is a special case of DR. The purpose of LPB is to minimize the effect of the relaxation of the created residual compressive stresses in the processed surface under a thermal overload. Thus, LPB is used for specific applications - most commonly for the treatment of gas turbine blades.

Studies related to static burnishing processes are focused in three main areas:

a) Influence of the parameters of the respective process on SI;

b) Investigation of the exploitation properties of the treated surfaces;

c) Investigation of the physical nature of the respective process.

The studies on smoothing burnishing processes are focused mainly on the final roughness and geometric accuracy. The objective in the study of deep burnishing processes is to investigate the final residual stress distribution and micro-hardness as they determine to a significant extent the exploitation behavior of the treated surfaces. The literature review shows that the basic approach to investigating static burnishing processes is the experimental approach [5-10]. This approach is undisputed when exploitation properties are being explored – fatigue behavior, wear resistance, crack resistance, corrosion resistance and more. On the other hand, the experimental approach is expensive and time consuming. When the subject of a study is the characteristics of SI, an alternative to the experimental approach is numerical simulation via the finite element method (FEM). FE simulations are a powerful tool for thoroughly studying the stressed and strained state in the surface and subsurface layers (including the useful residual stresses introduced through burnishing). Although the aspiration of each researcher is to develop an FE model to predict the most reliable results, different strategies have been applied to build an FE model of a static burnishing process. On the other hand, the FE model can predict not only the formation of some SI characteristics (for instance, residual stresses), but also to predict certain aspects of the operating behavior of the surface treated (for instance, residual stress relaxation caused by temperature, overloading or cyclic loading).

The purpose of this article is to systematically review the existing strategies for creating FE models of static burnishing processes and, on this basis, summarize the conditions for building an adequate FE model in correlation with the predicted characteristics of the respective burnishing process.

2. LITERARY SURVEY OF FE SIMULATIONS OF BURNISHING PROCESSES

Ever since the 1920s, research in static burnishing methods has been based on experimental investigations. With the development of FEM and computational techniques, at the end of the 20th century FE simulations of the burnishing processes [11-80] became an alternative to the experimental approach. One of the first studies on ball burnishing using an FE simulation was conducted by Skalski et al. [72]. In the following years, FEM established itself as an effective tool for studying burnishing processes. The research groups contributing FE simulations of burnishing processes include: RWTH Aachen University, Germany [13, 36, 65, 76]; Universite de Savoie, France [14, 15]; IMT, Szszecin, Poland [28-30]; Nanyang Technological University, Singapore [40, 41]; Saarland University, Saarbruecken, Germany [45, 46]; Bu-Ali Sina University, Iran [47, 48]; The Ohio State University, USA [69, 70, 78]; Air Vehicles Division, Melbourne, Australia [80] and the Technical University of Gabrovo, Bulgaria [53-56]. Some numerical studies by other researchers have

also been reported worldwide [11, 12, 16-27, 31-35, 37-39, 42-44, 49-52, 57-64, 66-68, 71, 73-75, 77, 79].

The general characteristics of the developed FE models are depicted in Table 1. Figure 3 shows that many more publications are devoted to the static burnishing methods incorporating rolling contact in comparison with SB. In terms of the rolling contact, the greatest attention is paid to the DR process (Fig. 4), followed by BB and RB. Figure 5 indicates that more than half of the studies are devoted to steel processing. When considering the group of non-ferrous materials, the greatest attention is paid to titanium alloys, followed by aluminum alloys. More than half of the FE models are three-dimensional (3D) (Fig. 6), which can be explained by the 3D nature of the static burnishing methods. Nevertheless, about one-third of the FE models are two-dimensional (2D) since the use of a 2D model shortens procedures, thus saving time. In a relatively small number (14.3%) of the publications, both types 2D and 3D FE models were used to compare the FE results obtained. While there is complete consensus about the behavior of the workpiece material, researchers have different viewpoints in terms of modeling the deforming element (Fig. 7). In just over half of the studies, the deforming element was modeled as a deformable solid. In 42.9% of the publications, an undeformable deforming element was preferred. In isolated cases, a deformable shell, as well as the replacement of the deforming element with additional boundary conditions on the workpiece, was preferred. In two-thirds of the studies (Fig. 8), the surface treated in 3D FE models was a plane facilitating the modeling of the kinematics. An outer cylindrical surface was a subject of 28.8% of the studies, while only 5.8% of the studies were dedicated to cylindrical openings. Figure 9 shows the relative weight of the models of the deforming element motion with respect to the static workpiece. The most commonly used models are F.2 and F.4 (see Table 1). It is noteworthy that, in a substantial number of studies, this important component of the FE model is not clear. It should be noted that F.1, F.2, F.3 and F.6 refer to simplified FE models. In almost two-thirds of the studies, the initial roughness (before burnishing) is not included in the FE model (Fig. 10). However, neglecting the initial roughness will not give good FE results for the surface layer. The vast majority of FE models are also temperature independent (Fig. 11). Figure 3 providess an explanation of this fact – modeling is being done of burnishing methods with rolling contact, in which the heat generated by friction is negligible. In more than half of the publications, the subject of study is residual stress distribution in the workpiece, introduced via the relevant process (Fig. 12). The explanation for this choice of subject is that reliable experimental determination of the residual stresses (for instance, via the X-ray diffraction technique) is time consuming and expensive; therefore, FEM is a preferred alternative. It makes an impression that a relatively large proportion of FE studies are devoted to the final roughness, although the experimental determination of roughness is not a problem. On the other hand, FE studies are also devoted to the determination of quantities that are very difficult to measure experimentally – for instance, the heat generated in the contact field in slide burnishing. The most commonly used software is ABAQUS, followed by ANSYS and Deform 2D (Fig. 13).

The characteristics of the material constitutive models in FE models are shown in Table 2. The constitutive model of the processed material is a very important component of the FE model. In 72.9% of the studies (Fig.14), the constitutive model was obtained on the basis of a one-dimensional (1D) test of the bulk material. Although the burnishing process affects the surface layers, the indentation test was used in only 8.6% of the studies. It is noteworthy that in almost one-fifth of the cases, the authors do not provide information on this very important issue. Figure 15 shows the types of 1D tests, providing information on building a constitutive model. The tensile test is the most popular. In more than one-third of the publications, this issue has not received even a comment. Most often (Fig. 16), the constitutive model is temperature and rate independent. It should be noted that the relatively high percentage of temperature-dependent models is due to the Johnson-Cook model, which does not mean that a thermal-mechanical FE analysis has been performed. Although the loading of the surface layers in the burnishing processes is cyclical, in almost half of the studies, isotropic strain hardening is used (Fig.17). In nearly one-third of the publications, this issue is not discussed by the authors, regardless of its importance, i.e., no mention has been made of the variation in the yield surface in the stress space, which is reflected in the residual stress distribution. Figure 18 shows how isotropic strain hardening of the bulk material is defined. Most often the Johnson-Cook model was used, followed by stress-strain data from the multilinear curve. A constant rate of expansion of the yield surface (bilinear curve) in the stress space was defined in 12.9% of the studies.

Table 1 *General characteristics of the FE models used*

Characteristic	Variants	Reference
A. Modeled process	A.1. Low plasticity burnishing	[11, 17, 27, 32, 39, 57, 80]
	A.2.Deep rolling	[12, 13, 16, 24, 26, 33, 40-42, 45-48, 50-52, 58, 61, 64, 65, 76, 77]
	A.3. Roller burnishing	[14, 22, 25, 31, 36, 37, 49, 59, 60, 68-70]
	A.4. Ball burnishing	[15, 18, 19-21, 23, 28-30, 44, 63, 66, 71-74, 78, 79]
	A.5. Slide burnishing	[34, 38, 53-56, 62, 67]
	A.6. Cryogenic burnishing	[35]
	A.7. Ultrasonic surface rolling process	[43]
	A.8. Ultrasonic assisted slide burnishing	[75]
B. Processed material	B.1. High-strength aluminium alloys	[11, 16, 22, 32, 35, 44, 48, 62, 75]
	B.2. Titanium alloys	
	B.2.1. Ti-6Al-4V	[17, 34, 36, 40-42, 50-52, 57, 63]
	B.2.2Ti-6Al-7Nb	[71]
	B.3. Magnesium alloy (AZ31B)	[77]

	B.4. Aluminium	[25, 49, 68]
	B.5. Nickel-titanium alloy (SE508)	[27]
	B.6. Brass (C38500)	[58]
	B.7. Biomaterial (MgCa0.8)	[66]
	B.8. Cast iron	[12, 21, 26]
	B.9. Steels	
	B.9.1. Inconel 718	[39, 80]
	B.9.2. Bearing steel (AISI 52100)	[31, 65, 69, 70, 78]
	B.9.3. Rail steel (R260; 76 steel)	[54]
	B.9.4. Medium carbon steel	[18-20, 23, 37, 60, 64, 67, 72]
	B.9.5. Low alloy steel	[24, 28-30, 33, 38, 43, 45, 46, 53, 55, 56, 61]
	B.9.6. Low carbon steel	[14, 15, 25]
	B.9.7. Micro alloy steel	[73]
	B.9.8. Nickel-chromium steel	[47]
	B.9.9. Tool steel (AISI D3)	[74]
C. Dimension of the FE model	C.1. 2D	[16, 18, 19, 22, 24, 25, 31, 34, 35, 37, 38, 44, 49, 56, 58, 62, 64, 66, 72-74]
	C.2. 3D	[11-15, 20, 23, 26-30, 32, 33, 36, 39, 40-43, 45-48, 50-53, 55, 57, 60, 61, 63, 67, 75-77, 79, 80]
	C.3. 2D+3D	[17, 21, 54, 59, 65, 68-71, 78]
D. Deforming element model	D.1. Rigid (Analytical rigid; Discrete rigid)	[12, 15-17, 26, 27, 31, 33, 38, 39, 42, 46, 48, 50, 54-56, 58, 61, 62, 65, 66, 69, 71, 72, 77, 78,
	D.2. Deformable solid	[11, 14, 18, 19, 20, 21, 23, 24, 28-30, 32, 34, 35, 37, 40, 41, 43-45, 51-53, 57, 59, 60, 64, 67, 68, 74, 75, 76, 80
	D.3. Deformable shell	[63]
	D.4. Without deforming element	[22, 25]
E. Processed surface in 3D models	E.1. Outer cylindrical	[14, 19, 20, 21, 26, 48, 56, 59, 60, 61, 63, 67, 68, 71, 76]
	E.2. Inner cylindrical (hole)	[53, 54, 55]
	E.3. Plane	[11-13, 15, 17, 18, 23, 27, 28-30, 32, 33, 36, 39, 40-43, 45-47, 50-52, 57, 65, 69, 70, 75, 77-80]
F. Movement of the tool relative to the workpiece	F.1 Normal loading – unloading (one cycle)	[20, 21, 28, 37, 59, 72]
	F.2. Normal loading – unloading – moving with magnitude equal to feed rate (type of "Rötger")	[16, 18, 34, 36, 54, 58, 62-67, 69-71, 73, 78]
	F.3. 2D pure rolling (in a straight line)	[17, 24, 31, 35, 74]
	F.4. 3D pure rolling (on a plane)	[12, 15, 17, 23, 26, 27, 29, 30, 32, 33, 40, 41, 42*, 43, 45, 50-52, 57, 77, 80]
	F.5. 3D pure rolling (on a cylindrical surface – circumferential direction)	[14, 48, 60, 61, 76]
	F.6. 2D sliding (in a straight line)	[38, 56**]
	F.7. 3D sliding (on a plane)	[11***]
	F.8. 3D sliding (on a cylindrical surface – circumferential direction)	[53, 54, 55]
	F.9. No tool defined	[22, 49]
	F.10. It is not clear	[25, 39, 44, 46, 47, 68, 75, 79]
G. Modeling of the initial roughness	G. 1. Yes	[14, 15, 18, 19, 23, 25, 29, 30, 37, 39, 44, 49, 53-56, 60, 62, 64-67, 69, 70, 73, 74, 78]
	G.2. No	[11, 12, 16, 17, 20-22, 24, 26-28, 31-36, 38, 40-43, 45-48, 50-52, 57-59, 61, 63, 68, 71, 75-77, 79, 80]
	G.3. It is not clear	[72]
H. Type of the FE analysis	H.1. Temperature-independent	[11-22, 24-31, 33, 34, 36-52, 54-80]
	H.2. Thermal-mechanical	[32, 35]
	H.3. Fully coupled thermal-stress	[23, 53]
I. Investigated feature of the	I.1. Displacements	[12, 28, 37, 38, 40, 59, 72, 73]

surface or process	I.2. Roughness	[14, 18-20, 22, 25, 44, 49, 56, 62, 69, 70, 74, 78]
	I.3. Accuracy of the form	[14, 15]
	I.4. Strains	[16, 17, 26-28, 31, 37-39, 56, 57, 79]
	I.5. Equivalent plastic strain	[12, 15, 31, 43, 59, 60, 71, 77]
	I.6. Equivalent stress	[59, 68]
	I.7. Residual stresses	[11-13, 16-21, 23-27, 29-34, 36-43, 45-58, 61, 63-67, 69-71, 74-78, 80]
	I.8. Residual stress relaxation	[17]
	I.9. Hardness	[77]
	I.10. Temperature	[35, 53]
	I.1.1. Burnishing force	[35, 42]
J. Software used	J.1. ABAQUS	
	J.1.1. Explicit solver	[26, 27, 33, 42, 43, 45, 46, 48, 50-52, 57, 66, 75, 76]
	J.1.2. Implicit solver	[12, 14, 15, 36, 40, 41, 53-56, 71, 80]
	J.1.3. Not mentioned	[21, 24, 31, 32, 58]
	J.2. Marc	[17, 23, 39]
	J.3. Zebulon	[18, 19]
	J.4. ANSYS	[22, 25, 37, 38, 44, 49, 59, 64, 67, 68, 73, 77, 79]
	J.5. NASTRAN	[28, 29, 30]
	J.6. Deform 2D	[34, 35, 65, 69, 70, 74, 78]
	J.7. Authorial software	[60]
	J. Not mentioned	[11, 16, 20, 47, 61, 62, 63, 72]

*Rotating the tool around two mutually perpendicular axes.
**The tool performs plane motion - superposition of translation and rotation.
***It is not explained in the text whether it's rolling or sliding. Given the shape of the deforming element in Fig. 2, however, it is obviously a sliding.

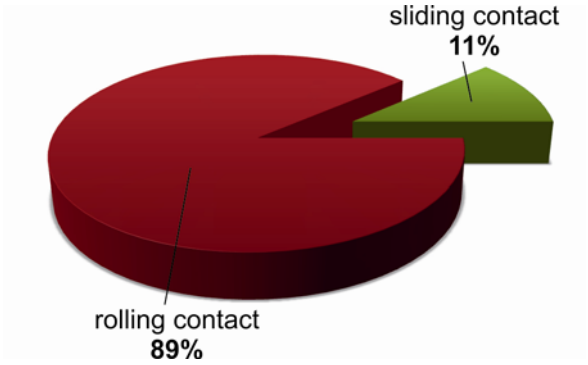

Fig. 3. Percentage share of the sliding friction and rolling contact

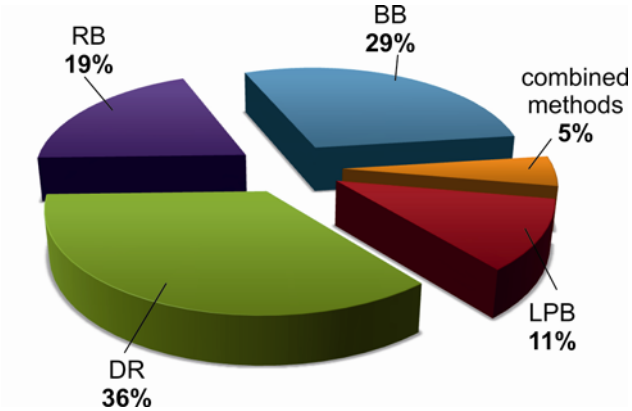

Fig. 4. Percentage share of the modeled processes with rolling contact

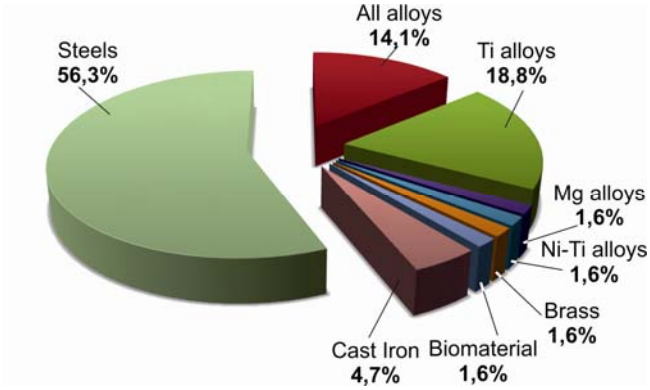

Fig. 5. Percentage share of the treated material

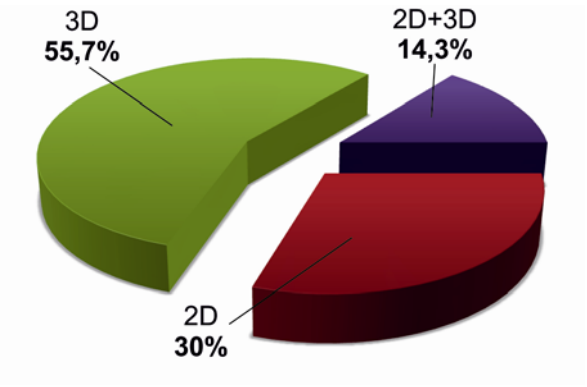

Fig. 6. Percentage share of 2D and 3D FE models

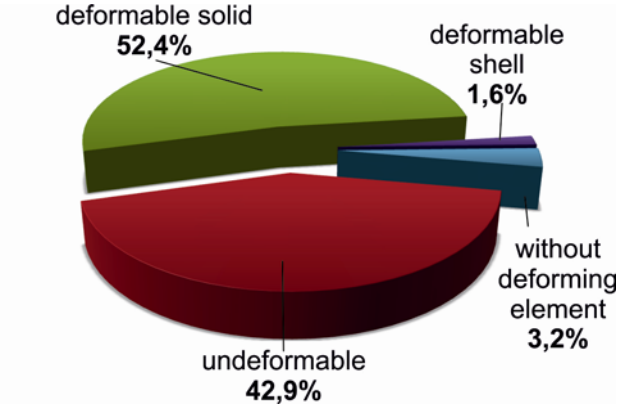

Fig. 7. Percentage share of the strategies for modeling of the deforming element

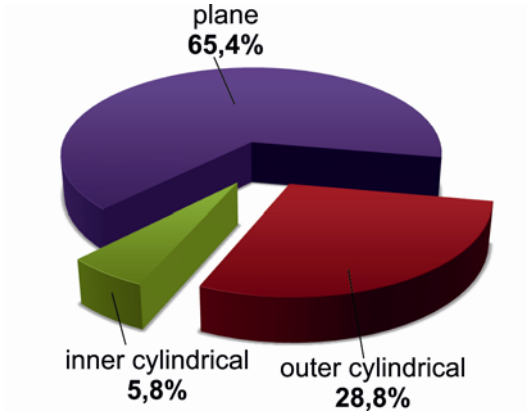

Fig. 8. Percentage share of the surfaces being treated in the FE models

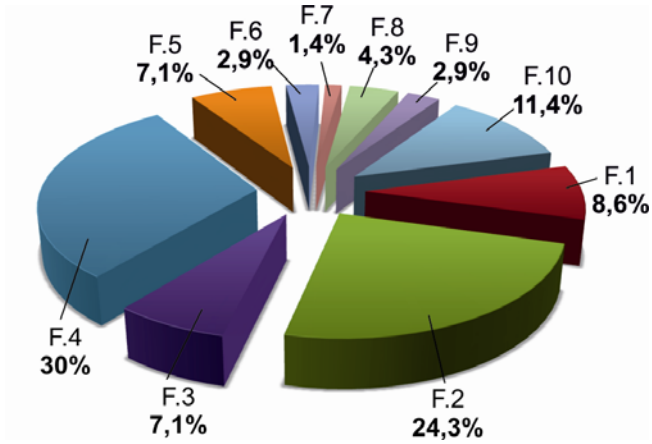

Fig. 9. Percentage share of the strategies for modeling of the motion in tool-workpiece system

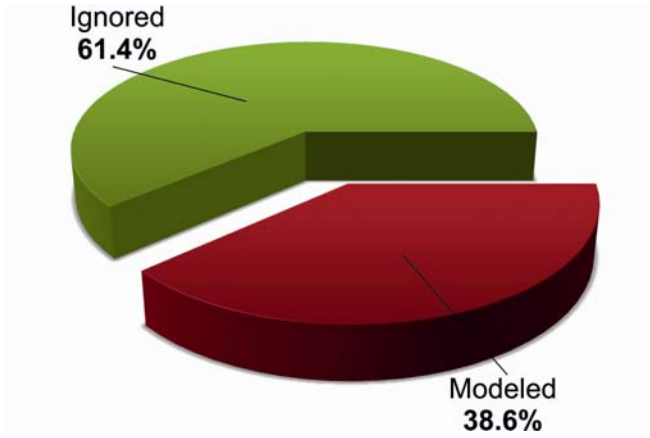

Fig. 10. Percentage share of the FE models according to "initial roughness" criterion

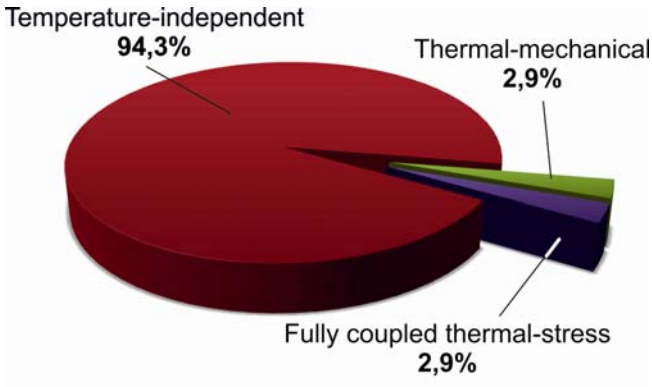

Fig. 11. Percentage share of the FE models depending on the temperature factor

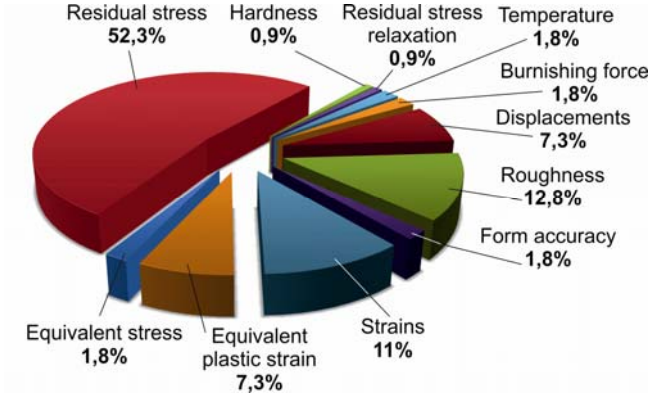

Fig. 12. Percentage share of the studied SI components

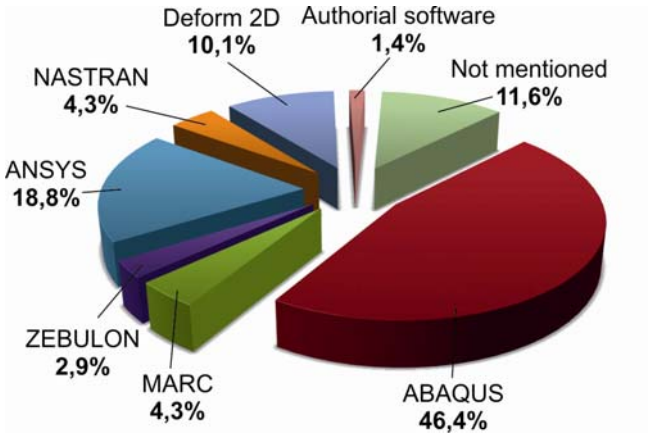

Fig. 13. Percentage share of the software used

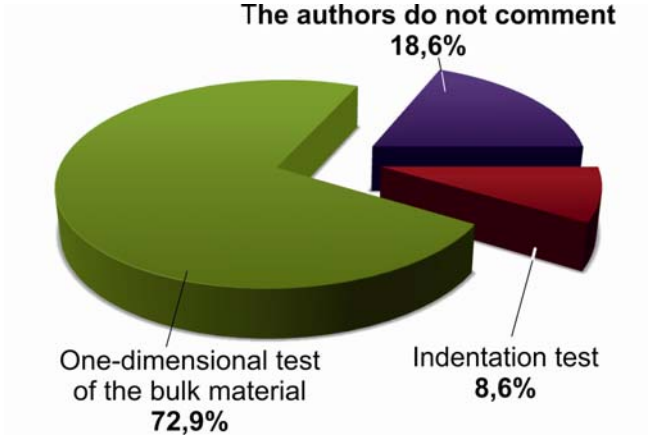

Fig. 14. Percentage share of the methods for obtaining constitutive model

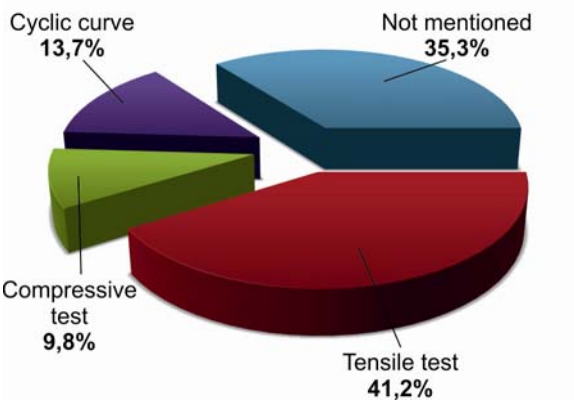

Fig. 15. Percentage share of the types of one-dimensional test

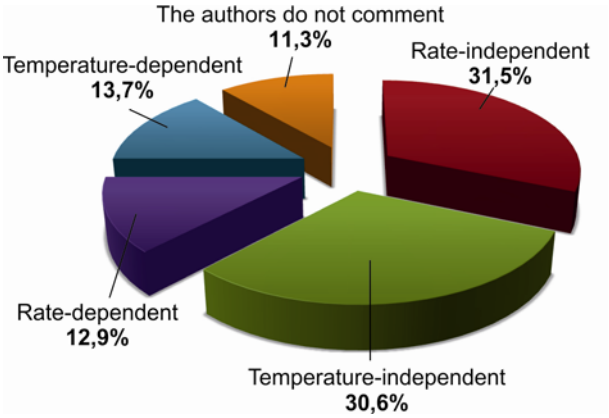

Fig. 16. Percentage share of the types of constitutive models

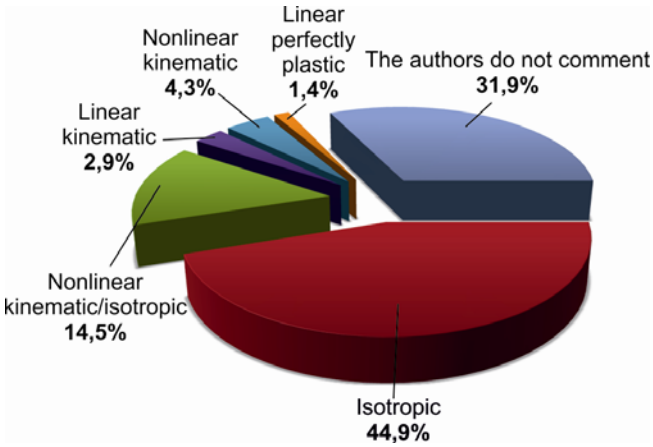

Fig. 17. Percentage share of the type of strain hardening in the used constitutive models

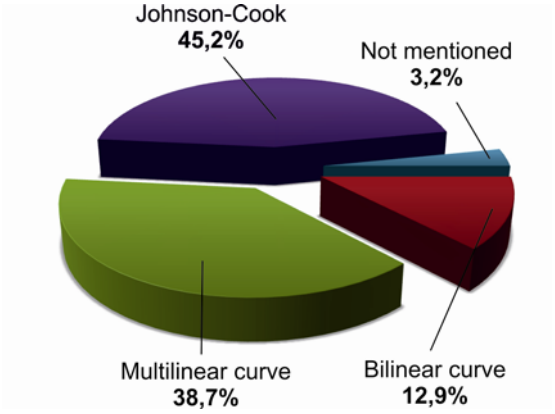

Fig. 18. Percentage share of the methods to define isotropic hardening

Table 2 *Characteristics of the constitutive model*

Characteristic	Variants	Reference
A. Obtained on the basis of:	A.1. Indentation test	[38, 53, 55, 56, 69, 70]
	A.2. One-dimentional test of the bulk material	
	A.2.1. Tensile test	[11, 18-21, 23, 24, 26, 28, 29, 34, 37, 41, 45, 54, 58, 64, 65, 67, 77, 78]
	A.2.2. Compressive test	[12, 14, 15, 26, 40]
	A.2.3. Cyclic curve (tension-compression)	[16, 33, 43, 48, 61, 76, 80]
	A.2.4. Not mentioned	[27, 31, 32, 35, 36, 39, 42, 46, 47, 50-52, 57, 63, 66, 71, 74, 75]
	A.3. It is not clear (The authors do not comment)	[17, 22, 25, 30, 44, 49, 59, 60, 62, 68, 72, 73, 79]
B. Type of the constitutive model	B.1. Rate independent	[11-16, 18, 19, 21, 24, 26-29, 31, 33, 34, 36-38, 40, 41, 43, 45, 46, 48, 53-56, 58, 61, 64, 67, 69-71, 76, 80]
	B.2. Temperature independent	[11-16, 18-21, 24, 26-29, 31, 33, 34, 36-38, 40, 41, 43, 45, 46, 48, 56, 58, 61, 64, 67, 69-71, 76, 77, 80]
	B.3. Rate dependent	[20, 23, 32, 35, 39, 42, 47, 50-52, 57, 63, 65, 66, 74, 78]
	B.4. Temperature dependent	[23, 32, 35, 39, 42, 47, 50-53, 55, 57, 63, 66, 74, 75, 77]
	B.5. It is not clear (The authors do not comment)	[17, 22, 25, 30, 44, 49, 59, 60, 62, 68, 72, 73, 75, 79]
C. Strain hardening	C.1. Isotropic	
	C.1.1. Bilinear curve	[11, 37, 64, 67]
	C.1.2. Stress-strain data	[14, 15, 18-20, 23, 26, 33, 38, 58, 65, 78]
	C.1.3. Johnson-Cook	[32, 35, 39, 42, 47, 50-52, 57, 63, 66, 74, 75, 77]

	C.1.4. Not mentioned	[71]
	C.2. Nonlinear kinematic/isotropic	[31*, 36, 43, 48, 53-56, 61, 76, 80]
	C.3. Linear kinematic	[45, 46]
	C.4. Nonlinear kinematic	[12, 16, 54]
	C.5. Linear perfectly-plastic behaviour	[24]
	C.6. It is not clear (The authors do not comment)	[17, 21, 22, 25, 27-30, 34, 40, 41, 44, 49, 59, 60, 62, 68-70, 72, 73, 79]
*The author claims that nonlinear isotropic hardening was used, but Eq. (3) shows the back stress tensor, i.e. nonlinear kinematic component.		

3. CONDITIONS FOR AN ADEQUATE FE MODEL

Based on Tables 1 and 2, the following generalization can be made. To build an adequate FE model of the static burnishing process, five basic conditions are necessary:

(1) Realistic geometries of the workpiece-modeled portion and the deforming element;

(2) An adequate constitutive model of the surface and the subsurface layers, where the model should be established in a manner that corresponds to the actual loading of these layers;

(3) A realistic interaction between the deforming element and the workpiece-modeled portion;

(4) Adequate boundary conditions, both geometrical and physical;

(5) An appropriate creation of the FE mesh.

3.1. Geometry of the deforming element – workpiece system

Our experience with the experimental determination of the residual stresses introduced by burnishing has shown that these stresses remain practically constant when the overall dimensions of the specimen are reduced via material removal. Hence the overall dimensions of the workpiece-modeled portion can be on the order of $5 \div 7mm$. The modeling of the initial roughness is a mandatory condition for producing a realistic geometry, since the burnished surface layer is characterized by severe equivalent plastic deformation. However, the micro-profile of the roughness has a stochastic character, while the FEM generally requires a determined geometry of the field of integration. A known solution [67] is to scan the roughness micro-profile of a machined specimen and enter the information into the FE software used. A compromise can be reached by modeling the initial kinematic roughness based on the feed rate (in the turning process) and the roughness height R_z. Replacing the deforming element with assigned boundary conditions (geometrical and physical) in the contact area of the workpiece-modeled portion is not a good idea because the FE model becomes over-simplifies. Modeling the exact geometry of the deforming element is an important condition for assigning adequate interactions to the tool-workpiece system.

3.2. Material constitutive model of the workpiece-modeled portion

Of the above five prerequisites for obtaining a reliable FE model, the most responsive and labor-intensive one concerns the material constitutive model. The surface layer of the workpiece is what the burnishing process acts upon. Normally, the behavior of this surface layer differs considerably from that of the bulk material due to the presence of large plastic strains and specific micro-profiles, as well as other effects due to the workpiece production. Due to this difference, conventional testing methods for stress–strain curve determination using a 1D (compressive, tensile or cyclic) test can be applied readily to the bulk material but not to the surface layer, as they are not suitable for the surface layer. The dependence between the stress and strain tensors in the plastic field of the surface layer must be determined in correspondence to the actual loading of this layer. It is appropriate to use an instrumented indentation test together with an FE inverse analysis, as doing so will allow the acquisition of the local load–deformation responses at the surface. For some materials, it is advisable that the indentation test be conducted under the conditions of a stabilized cycle [81]. SB has a thermo-mechanical nature. Therefore, the constitutive model of the surface layers should be temperature dependent when an SB process is modeled. In other words, the indentation test should be conducted under different temperatures [53]. The burnishing process causes cyclic loading in the vicinity of a point from the surface layer of the workpiece. The cyclic external load causes the structure of the material to change on a micro-level, which is reflected in the alteration of the material's behaviour in terms of strain hardening. Therefore, the strain hardening should contain a kinematic component. A nonlinear kinematic hardening component describes the translation of the yield surface in the stress space through the back-stress tensor, while an isotropic hardening component describes the change in the equivalent stress defining the size of the yield surface as a function of the plastic deformation. In other words, the kinematic hardening component predicts the plastic shakedown after one cycle, while the material plastic behavior after several cycles is predicted by combined hardening (the isotropic component combined with the nonlinear kinematic component). However, in [81], it was shown that, for some steels, the criterion for achieving a stabilized cycle of surface being burnished is the number of passes, but no cyclic loading coefficient, i.e., no cyclic hardening occurs when burnishing is conducted in one pass. This means that if burnishing process with one pass is simulated, just a nonlinear kinematic hardening component may be sufficient. Hence, it is necessary that the adequacy of the constitutive model be proven by comparing the FE results (residual stresses) with the experimental ones (for example, via the X-ray diffraction technique).

3.3. Interactions between the deforming element and the workpiece-modeled portion

The contact between the deforming element and the surface being burnished is both mechanical and thermal (heat generation). The mechanical contact is normal (allowing separation after contact) and tangential with the defined friction coefficient. Due to the thermal-mechanical nature of the SB process, the reliable determination of this coefficient is of great importance for the accuracy of the FE results obtained. As established in [82], the friction coefficient in the SB process depends strongly on the

process parameters. In contrast, the burnishing methods using rolling contact are significantly less affected by the friction. The assignment of an adequate thermal contact (heat generation) is of much greater importance to SB than to burnishing with rolling contact.

3.4. Boundary conditions

The boundary conditions are geometrical and physical (mechanical and thermal), as the thermal component is of no practical significance in burnishing with rolling contact. Usually the burnishing of rotational surfaces is accomplished by the workpiece rotating about a fixed axis, with the deforming element performing the translation (or superposition of translation and rotation) in order to ensure the continuity of the deformation process. In the FE simulations, the inversion method is used, i.e., a reverse angular velocity is applied to the tool-workpiece system. As a result, the workpiece becomes stationary and the deforming element receives an additional angular velocity. Therefore, the boundary conditions of the workpiece-modeled portion must perform an appropriate fixation (as an ideal rigid body), and the impact of the removal of part of the workpiece must be taken into account (for instance, by assigning an elastic foundation). The boundary conditions for the deforming element must provide the necessary relative movement towards the workpiece-modeled portion in order to ensure: 1) a defined contact between the deforming element and the surface being burnished; 2) the magnitudes of the process parameters, i.e., burnishing force, feed rate and burnishing velocity. The thermal boundary conditions must provide for adequate heat generation due to friction and plastic deformation, as well an adequate heat transfer.

3.5. FE mesh

Since the burnishing creates a very high gradient of the strains in the normal direction (with respect to the surface layer), a very fine mesh near the surface should be used. It should be noted that the sizes of the FEs on the surface must be consistent with the correct description of the initial roughness. Since the material at depth remains unaffected, the FE mesh in the direction of the core should be coarser.

4. CONCLUSIONS AND PERSPECTIVES

Based on the review the following conclusions can be made:

- With the development of FEM and computational techniques, FE simulations of the static MST processes have become an alternative and natural addition to the experimental approach. The development of FEM is in direct correlation with the development of high-speed computers. Looking forward, the modeling the entire burnishing process (including the object geometry, number of passes and so on) will become a reality.
- To build an adequate FE model of the static burnishing process, five basic conditions are necessary: realistic geometries of the workpiece-modeled portion and the deforming element; an adequate constitutive model of the surface and the subsurface layers, where the model should be established in a manner that corresponds to the actual loading of these layers; a realistic interaction between the deforming element and the workpiece-modeled portion; adequate boundary conditions both geometrical and physical; and an appropriately created the FE mesh.
- The constitutive model of the surface and subsurface layers is critical to producing an adequate FE model. It is important to note that the constitutive model is valid for the particular material on which the corresponding test has been carried out. The surface layer of the workpiece is what the burnishing process acts upon. The dependence between the stress and strain tensors in the plastic field of the surface layer and subsurface layers must be determined in correspondence to the actual loading of the surface layer. It is appropriate to use an instrumented indentation test together with an FE inverse analysis, as doing so will allow the acquisition of the local load–deformation responses at the surface. In static MST processes, the elementary volume in the vicinity of each point (that contacts the deforming element) on the treated surface is subjected to cyclic loading, which provokes deformation anisotropy, i.e., the yield surface is expanded and moved irregularly into the space of the stresses. Therefore, the strain hardening should contain a nonlinear kinematic component. However, it is necessary to validate the constitutive model by comparing the FE results with the experimental results.

REFERENCE

[1] Maximov J.T., Duncheva G.V., Anchev A.P., Ichkova M.D. Slide burnishing – review and prospects. International Journal of Advanced Manufacturing Technology (2019) https://doi.org/10.1007/s00170-019-03881-1

[2] Ecoroll Catalogue “Tools and solutions for metal surface improvement”. Ecoroll Corporation Tool Technology, USA, 2006.

[3] Prevey P. Burnishing and apparatus for providing a layer of compressive residual stress in the surface of a workpiece. US Patent 5826453, Patented Oct. 27, 1998

[4] Prevey P. Method and apparatus for providing a residual stress distribution in the surface of a part. US Patent 6415486, Patented Jul. 9, 2002

[5] Amdouni H., Bouzaine H., Montagne A., Van Gorp A., Coorevits T., Nasri M., Iost A. Experimental study of a six new ball-burnishing strategies effects on the Al-alloy flat surfaces integrity enhancement. Int J Adv Manuf Technol 90 (2017) 2271-2282

[6] Yuan X., Sun Y., Li C., Liu W. Experimental investigation into the effect of low plasticity burnishing parameters on the surface integrity of TA2. Int J Adv Manuf Technol 88(1-4) (2017) 1089-1099

[7] Vukelic D., Tadic B., Dzinic D., Kocovic V., Brzakovic L., Zivkovic M., Simunovic G. Analysis of ball-burnishing impact on barrier properties of wood workpieces. Int J Adv Manuf Technol 92(1-4) (2017) 129-138

[8] Bounoura A., Hamadache H., Amirat A. Investigation on the effect of ball burnishing on fracture toughness in spiral API X70 pipeline steel. Int J Adv Manuf Technol 94(9-12) (2018) 4543-4551

[9] Tang J., Luo H.Y., Zhang Y.B. Enhancing the surface integrity and corrosion resistance of Ti-6Al-4V titanium alloy through cryogenic burnishing. Int J Adv Manuf Technol 88(9-12) (2017) 2785-2793

[10] Amdouni H., Bouzaine H., Montagne A., Nasri M., Iost A. Modeling and optimization of a ball-burnished aluminum alloy flat surface with a crossed strategy based on response surface methodology. Int J Adv Manuf Technol 88(1-4) (2017) 801-814

[11] Aldrine M.E., Mahendra Babua N.C., Anil Kumara S. Evaluation of induced residual stresses due to low plasticity burnishing through finite element simulation. Materials Today: Proceedings 4 (2017) 10850–10857

[12] Ali M., Michlik P., Pan J. Residual stress distributions in rectangular bars due to high rolling loads. SAE International Journal of Materials and Manufacturing 9 (3) (2016) 661-678

[13] Bäcker V., Klocke F., Wegner H., Timmer A., Grzibovskis R., Rjasanow S. Analasys of deep rolling process on turbine blades using FEM/BEM-coupling. IOP Conference Series: Materials Science and Engineering 10 (2010) 1-10

[14] Balland P., Tabourot L., Degre F., Morean V. An investigation of the mechanics of roller burnishing through finite element simulation and experiments. International Journal of Machine Tools and Manufacture 65 (2013) 29-36

[15] Balland P., Tabourot L., Degre F., Moreau V. Mechanics of the burnishing process. Precision Engineering 37(2013)129-134

[16] Beghini M., Bertini L., Monelli B.D., Santus S., Bandini M. Experimental parameter sensitivity analysis of residual stresses induced by deep rolling on 7075-T6 aluminium alloy. Surface and Coatings Technology 254 (2014) 175-186

[17] Beres W., Patnaik P., Li J. Numerical simulation of the low plasticity burnishing process for fatigue property enhancement. Proceedings of the ASME Turbo Expo 2004, Power and Land, Sea and Air, June 14-17, 2004, Vienna, Austria

[18] Bougharriou A., Bouzid W., Saï K. Prediction of surface characteristics obtained by burnishing. International Journal of Advanced Manufacturing Technology 51 (2010) 205-215

[19] Bougharriou A., Saï K., Bouzid W. Finite element modelling of burnishing process. Materials Technology 25 (1) (2010) 56-62

[20] Bouzid Sai W., Sai K. Finite element modeling of burnishing of AISI 1042 steel. International Journal of Advanced Manufacturing Technology 25 (2005) 460-465

[21] Courtin S., Henaff-Gardin C., Bezine G. Finite element simulation of roller burnishing in crankshafts. Transactions on Engineering Sciences 39 (2003) 333-342

[22] Dadmal S., Kurkute V. Finite Element Analysis of Roller Burnishing Process. International Research Journal of Engineering and Technology 4 (6) (2017) 2294-2301

[23] Deng W.J., Xia W., Zhou Z.Y., Chen W.P., Li Y.Y. Finite Element Analysis of Effects of Ball Burnishing Parameters on Residual Stresses. Materials Science Forum 471-472 (2004) 658-662

[24] Donzella G., Guagliano M., Vergani L. Experimental investigation and numerical analyses on deep rolling residual stresses. Transaction on Engineering Sciences 2 (1993) 13-27

[25] Eshwara Prasad K., Nahavandi S., Mohammed M., Aditiya V. Prediction of Residual Stresses in Roller Burnished Components – A Finite Element Approach. International Journal of Applied Engineering Research 1 (2) (2006) 153-163

[26] Fonseca L., de Faria A. A deep rolling finite element analysis procedure for automotive crankshafts. Journal of Strain Analysis 53 (3) (2018) 178-188

[27] Fu C.H., Guo Y.B., McKinney J., Wei X.T. Process Mechanics of Low Plasticity Burnishing of Nitinol Alloy. Journal of Materials Engineering and Performance 21 (2012) 2607-2617

[28] Grochała D., Berczyński S., Grządziel Z. Modeling of burnishing thermally toughened X42CrMo4 steel with a ceramic ZrO_2 ball. Archives of Civil and Mechanical Engineering, 17 (4) (2017) 1011-1018

[29] Grochala D., Berczynski S., Grzadziel Z. Stress in the surface layer of objects burnished after milling. International Journal of Advanced Manufacturing Technology 72 (2014) 1655-1663

[30] Grochala D., Berczynski S., Grzadziel Z. Testing of the State of Stress after Finish Burnishing Items. Journal of Machine Construction and Maintenance 108 (2018) 45-52

[31] Guo Y.B., Barkey M.E. FE-simulation of the effects of machining- induced residual stress profile on rolling contact of hard machined components. International Journal of Mechanical Sciences 46 (2004) 371–388

[32] Hassanifard S., Mousavi M., Varvani-Farahani A. The influence of low-plasticity burnishing process on the fatigue life of friction-stir-processed Al7075-T6 samples. Fatigue and Fracture of Engineering Materials and Structures 42(3) (2019) 764-772

[33] Hassani-Gangaraj S., Carboni M., Gnagliano M. Finite element approach toward an advanced understanding of deep rolling induced residual stresses, and an application to railway axles. Materials and Design 83 (2015) 689-703

[34] He D., Wang B., Zhang J., Liao S., Deng W.J. Investigation of interference effect on the burnishing process. International Journal of Advanced Manufacturing Technology 95 (2018) 1-10

[35] Huang B., Kaynak Y., Sun Y., Jawahir I. Surface layer modification by cryogenic burnishing of Al7050-T7451 alloy and validation with FEM-based burnishing model. Procedia CIRP 31 (2015) 1-6

[36] Klocke F., Bäcker V., Wegner H., Zimmermann M. Finite element analysis of the roller burnishing process for fatigue resistance increase of engine components. Proceedings of the Institution of Mechanical Engineers, Part B: Journal of Engineering Manufacture 225 (1) (2011) 2-11

[37] Kulakowska A. Numerical analysis of the influence of surface asperity vertical angles after turning on the state of stress and strains after part's burnishing rolling. Logitrans - VII Konferencja Nankowo-Techniczka, 14-16 April, Szczyrk, Poland, 2010, pp. 1793-1802

[38] Kuznetsov V., Smolin I., Dmitriev A., Konovalov D., Makarov A., Kiryakov A., Yurovskikh A. Finite Element Simulation of Nanostructuring Burnishing. Physical Mesomechanics 16 (1) (2013) 62-72

[39] Li F.L., Xia W., Zhou Z. Y. Finite Element Calculation of Residual Stress and Cold-work Hardening Induced in Inconel 718 by Low Plasticity Burnishing. Third International Conference on Information and Computing, Wuxi, China, 4-6 June 2010

[40] Lim A., Castagne S., Wong C. Effect of deep cold rolling on residual stress distributions between the treated and untreated regions on Ti-6Al-4V alloy. Journal of Manufacturing Science and Engineering 138(11) (2016) 111005-111005-8

[41] Lim A., Castagne S., Wong C. Effect of Friction Coefficient on Finite Element Modeling of the Deep Cold Rolling Process. Proceedings of 12th International Conference on Shot Peening, 15-18 September, Goslar, Germany, 2014, pp. 376-380

[42] Liou J., El-Wardany T. Finite element analysis of residual stress in Ti-6Al-4V alloy plate induced by deep rolling process under complex roller path. International Journal of Manufacturing Engineering (2014) 1-14 http://dx.doi.org/10.1155/2014/786354

[43] Liu Y., Wang L., Wang D. Finite element modeling of ultrasonic surface rolling process. Journal of Materials Processing Technology 211 (2011) 2106-2113

[44] Loriya S.S., Patel V. Finite element analysis of ball burnishing process of aluminium alloy 6061-T6. International Journal of Advance Engineering and Research Development 5(3) (2018) 1105-1118

[45] Lyubenova N., Baehre D. Finite element modelling and investigation of the process parameters in deep rolling of AISI4140 Steel. Journal of Materials Science and Engineering 5(7-8) (2015) 277-287

[46] Lyubenova N., Jacquemin M., Bahre D. Influence of the Pre-Sressing on the Residual Stresses Induced by Deep Rolling. Materials Research Proceedings 2 (2016) 253-258

[47] Majzoobi, G.H., Motlagh, S.T., Amiri, A. Numerical simulation of residual stress induced by roll-peening. Trans. Indian Inst. Met. 63 (2010) 499–504

[48] Majzoobi G., Zare Jouneghani F., Khademi E. Experimental and numerical studies on the effect of deep rolling on bending fretting fatigue resistance of Al7075. International Journal of Advanced Manufacturing Technology 82(9-12) (2016) 2137-2148

[49] Malleswara Rao J.N., Chennakesava Reddy A., Rama Rao P.V. Finite element approach for the prediction of residual stresses in aluminum work pieces produced by roller burnishing. International Journal of Design and Manufacturing Technology 2 (2011) 7-20

[50] Manouchehrifar A., Alasvand K. Finite element simulation of deep rolling and evaluate the influence of parameters on residual stress. Recent Researches in Engineering Mechanics, Urban & Naval Transportation and Tourism (2009) 61-67

[51] Manouchehrifar A., Alasvand K. Finite element simulation of deep rolling and evaluate the influence of parameters on residual stresses. Recent Researches in Applied Mechanics (2012) 121-127

[52] Manounchehrifar A., Alasvand K. Simulation and research on deep rolling process parameters. International Journal of Advanced Design and Manufacturing Technology 5(5) (2012) 31-37

[53] Maximov J.T., Duncheva G.V., Anchev A.P. A temperature-dependent, nonlinear kinematic/isotropic hardening material constitutive model of the surface layer of 37Cr4Steel subjected to slide burnishing. Arabian Journal for Science and Engineering (2019) DOI.org/10.1007/s13369-019-03765-2

[54] Maximov J.T., Duncheva G.V., Anchev A.P., Amudjev I.M., Kuzmanov V.T. Enhancement of fatigue life of rail-end-bolt holes by slide diamond burnishing. Engineering Solid Mechanics 2(4) (2014) 247-264

[55] Maximov J.T., Duncheva G.V., Anchev A.P., Dunchev V.P. Crack resistance enhancement of joint bar holes by slide diamond burnishing using new tool equipment. International Journal of Advanced Manufacturing Technology (2019) DOI.org/10.1007/s00170-019-03405-x

[56] Maximov J.T., Duncheva G.V. Finite Element Analysis and optimization of spherical motion burnishing of low-alloy steel. Proceedings of the Institution of Mechanical Engineers, Part C: Journal of Mechanical Engineering Science 226(1) (2012) 161-176

[57] Mohammadi F., Sedaghati R., Bonakdar A. Finite element analysis and design optimization of low plasticity burnishing process. International Journal of Advanced Manufacturing Technology 70(5-8) (2014) 1337-1354

[58] Mombeini D., Atrian A. Investigation of deep cold rolling effects on the bending fatigue of brass C38500. latin American Journal of Solid and Structures 15(4) (2018) e36 1-19

[59] Patabhi Reddy B., Shashikanth C. Investigations in contact stress analysis in roller burnishing process. International Journal and Magazine of Engineering, Technology, Managment and Research 2(11) (2015) 1502-1516

[60] Patyk S., Patyk R., Kukielka L., Kaldunski P., Chojnacki J. Numerical Method for Determining the Main Force of Burnishing Rolling of Rough Cylindrical Surface with Regular Periodical Outlines Asperities. 23rd International Conference Engineering Mechanics 2017, Svratka, Czech Republic, 15-18 May 2017 pp. 754-757

[61] Perenda, J., Trajkovski, J.,˘Zerovnik, A., Prebil, I. Residual stresses after deep rolling of a torsion bar made from high strength steel. J. Mater. Process.Technol. 218 (2015) 89–98

[62] Posdzich M., Stockmann R., Morczinek F., Putz M. Investigation of a Plain Ball Burnishing Process on Differently Machined Aluminium EN AW 2007 Surfaces. MATEC Web of Conferences 190, 11005 (2018), ICNFT 2018

[63] Revankar G., Shetty R., Rao S., Gaitonde V. Wear resistnace enhancemenet of titanium alloy (Ti-6Al-4V) by ball burnishing process. Journal of Materials Research and Technology 6(1) (2017) 13-32

[64] Rodríguez A., López de Lacalle L.N., Celaya A., Lamikiz A., Albizuri J. Surface improvement of shafts by the deep ball-burnishing technique. Surface and Coatings Technology 206 (2012) 2817–2824

[65] Röettger K. Walzen hartgedrehter oberflaechen, PhD Thesis, WZL, RWTH Aachen, University, Aachen, Germany, 2002

[66] Salahshoor M., Guo Y.B. Finite Element Modeling of Burnishing and the Effects of Process Parameters on Surface Integrity of Orthopedic Implants. Proceedings of the ASME 2011 International Mechanical Engineering Congress & Exposition IMECE2011 November 11-17, 2011, Denver, Colorado, USA

[67] Saldaña-Robles A., Aguilera-Gomez E., Plascencia-Mora H., Ledesma E., Reveles-Arredondo J., Saldaña-Robles N. FEM burnishing simulation including roughness. Mechanik 2 (2015) 79-91

[68] Saritha P. A. Study on assesment of theories for contact stress distribution at roller-work piece contact in roller burnishing. International Journal of Sciences, Engineering and Technology Research 3(1) (2014) 100-106

[69] Sartkulvanich P., Altan T., Jasso F., Rodriguez C. Finite element modeling of hard roller burnishing: An analysis on the effects of process parameters upon surface finish and residual stresses. J. Manuf. Sci. Engng. 129(4) (2007) 705–716

[70] Sartkulvanich P. Determination of material properties for use in FEM simulations of machining and roller burnishing. PhD Thesis, 2007

[71] Sayahi M., Sghaier S., Belhadjsalah H. Finite element analysis of ball burnishing process: comparisons between numerical results and experiments. International Journal of Advanced Manufacturing Technology 67(5-8) (2013) 1665-1673

[72] Skalski K., Morawski A., Przybylski W. Analysis of contact elastic-plastic strains during the process of burnishing. International Journal of Mechanical Sciences 37 (1995) 461–472

[73] Srinivasa Rao D., Haviprasad Rao P., Gopal Sekhar R. Evaluation of surface roughness of burnished dual -phase steels using experimental and finite element methods. International Journal of Current Engineering and Technology 3(4) (2013) 1375-1378

[74] Stalin John M.R., Welsoon Wilson A., Prasad Bhardwaj A., Abraham A., Vinayagam B.K. An investigation of ball burnishing process on CNC lathe using finite element analysis. Simulation Modeling Practice and Theory 62 (2016) 88-101

[75] Teimouri R., Amini S., Bami A.B. Evaluation of optimized surface properties and residual stress in ultrasonic assisted ball burnishing of AA6061-T6. Measurement 116 (2018) 129-139

[76] Trauth D., Klocke F., Mattfeld P., Klink A. Time-efficient prediction of thesurface layer state after deep rolling using similarity mechanics approach. Procedia CIRP 9 (2013) 29–34

[77] Uddin M.S., Hall C., Hooper R., Charrault E., Murphy P., Santos V. Finite element analysis of surface integrity in deep ball-burnishing of a biodegradable AZ31B Mg. Metals 136(8) (2018) 1-17

[78] Yen Y.C., Sartkulvanich P., Altan T. Finite element modeling of roller burnishing process. CIRP Annals 54(1) (2005) 237–240

[79] Zemcik O., Chladil J., Sedlak J. Changes in the surface layer of rolled bearing steel. Acta Polytechnica Journal of Advanced Engineering 55(5) (2015) 347-351

[80] Zhuang W., Wicks B. Multipass low-plasticity burnishing induced residual stresses: three-dimensional elastic-plastic finite element modeling. Proceedings of the Institution of Mechanical Engineers, Part C: Journal of Mechanical Engineering Science 218(6) (2004) 663-668

[81] Maximov J.T., Duncheva G.V., Anchev A.P., Ganev N., Dunchev V.P. Effect of cyclic hardening on fatigue performance of slide burnished components made of low-alloy medium carbon steel. Fatigue and Fracture of Engineering Materials and Structures (2019) DOI: 10.1111/ffe.13001

[82] Maximov J.T., Anchev A.P., Duncheva G.V. Modeling of the friction in tool-workpiece system in diamond burnishing process. Coupled Systems Mechanics 4 (4) (2015) 279-295